

The transmission factors  $T_{\mu}^{\text{HF}}$  were calculated with the same surface peaked absorptive potential  $W_D=5.0$  MeV used in Sec. III A for fitting the off-resonance cross sections. For the cases  $^{90}\text{Zr}$  and  $^{92}\text{Mo}$  with closed neutron channels, the lower absorption  $W_D=1.5$  appeared to be more appropriate.<sup>18,21</sup> The estimate  $W^{\text{int}} \leq 3.0$  keV for the internal spreading width was adopted.<sup>48</sup> Since both the enhancement factor  $f^2$  [Eq. (2)] and the external spreading width  $W_{\mu}^{\text{ext}}$  depend on the ratio  $\Delta_{\mu}^{\text{sp}}/\Gamma_{\mu}^{\text{sp}}$ , we review this quantity in Table V. Column 11 contains the values determined from the spreading widths using Eq. (7); column 10 those obtained from the  $(p, n)$  and  $(p, p_0)$  data.<sup>49</sup> The agreement between the two sets is surprisingly good in view of the fact that in both theories the continuum-continuum interaction has been neglected.<sup>50</sup>

### 5. CONCLUSION

Yield curves and angular distributions of  $\gamma$  rays produced in the reaction  $^{89}\text{Y}(p, n\gamma)^{89}\text{Zr}$  were measured over the  $s_{1/2}$  and  $d_{3/2}$  single-particle analog resonances in  $^{90}\text{Zr}$  at 6.1- and 7.4-MeV proton energy using a 56-cm<sup>2</sup> Ge(Li) detector. Neutron excitation functions were

<sup>48</sup> A. F. R. de Toledo Piza, A. U. Kerman, S. Fallieros, and R. H. Venter, Nucl. Phys. **89**, 369 (1966).

<sup>49</sup> The calculations of A. Mekjian (private communication) for the analogs of the  $d_{3/2}$  ground state in  $^{89}\text{Sr}$  and the  $s_{1/2}$  single-particle states in  $^{91}\text{Zr}$  and  $^{93}\text{Mo}$  yield an upper limit of  $W^{\text{int}}=1.0$  keV for the internal spreading width compared with  $W^{\text{int}}=3.0$  keV used throughout Table V. Adopting Mekjian's value, the ratios  $\Delta_{\mu}^{\text{sp}}/\Gamma_{\mu}^{\text{sp}}$  in column 11 change only by 5% except for the  $d_{5/2}$  IAR in  $^{89}\text{Sr}$ , where  $\Delta_{\mu}^{\text{sp}}/\Gamma_{\mu}^{\text{sp}} = -6.7$ .

<sup>50</sup> T. Tamura, Phys. Rev. (to be published).

obtained indirectly from the  $\gamma$ -ray yields by correcting them for the efficiency of the detector. The selective neutron decay of the resonances to states in  $^{89}\text{Zr}$  was found to be caused by the optical  $p$ -wave size resonance in the mass-90 region. This fact combined with the observed neutron branching ratios and  $\gamma$ -ray transitions and angular distributions made possible spin-parity assignments to a number of states in  $^{89}\text{Zr}$ . Evidence is given for a weak coupling multiplet of the structure [ $^{90}\text{Zr}(2^+)M_{\nu}^{-1}(g_{9/2})$ ].

The asymmetric resonance shapes of the 1628 $\rightarrow$ 0-, 1834 $\rightarrow$ 0-, and 2081 $\rightarrow$ 1093-keV transitions at the 6.16-MeV  $1^-$  analog state were analyzed in order to find the level shift  $\Delta$ . A comparison was made for available shifts of analogs of single-particle neutron states built upon some  $N=50$  isotones and  $Z=40$  isotopes. It was found that the level shifts derived from the  $(p, n)$  and  $(p, p_0)$  cross-section measurements agree reasonably well with those calculated from the external-spreading widths of these resonances.

### ACKNOWLEDGMENTS

The authors wish to thank Dr. T. Tamura, Dr. D. Robson, Dr. W. R. Coker, and Dr. E. Sheldon for stimulating discussions, Dr. P. Richard for making available the  $^{56}\text{Co}$  source, and Dr. P. Buchanan for communicating her results prior to publication. They gratefully acknowledge the hospitality extended to them by their colleagues at the Center for Nuclear Studies; one of them (K.P.L.) appreciates a Fulbright Fellowship granted by The University of Texas.

## Reorientation-Effect Measurements on $\text{Cd}^{114}\dagger$

J. X. SALADIN, J. E. GLENN,\* AND R. J. PRYOR

*Department of Physics, University of Pittsburgh, Pittsburgh, Pennsylvania 15213*

(Received 29 April 1969)

Using a 42-MeV  $\text{O}^{16}$  beam, the angular dependence of the excitation probability for exciting the first  $2^+$  state in  $\text{Cd}^{114}$  has been determined. The energy dependence of the same quantity was determined by means of an  $\alpha$  beam. From these data, the quadrupole moment  $Q_2^+$  of the first  $2^+$  state was determined, as well as the reduced transition probability  $B(E2, 0\rightarrow 2^+)$ . The two sets of data are consistent with each other and with particle- $\gamma$ -coincidence experiments of several other groups. A detailed account of the experimental techniques and the method of evaluation is given.

### I. INTRODUCTION

IN an earlier paper,<sup>1</sup> we reported preliminary results of quadrupole moment measurements of the first  $2^+$  state of  $\text{Cd}^{114}$ . These measurements were based on the so-called reorientation effect in Coulomb excitation and were carried out by means of an  $\text{O}^{16}$  beam. Experiments on  $\text{Cd}^{114}$  have been carried out by several

groups,<sup>2-7</sup> exploiting different aspects of the reorientation effect and using different experimental tech-

<sup>2</sup> J. de Boer, R. G. Stokstad, G. D. Symons, and A. Winther, Phys. Rev. Letters **14**, 564 (1965).

<sup>3</sup> J. J. Simpson, D. Eccleshall, M. J. L. Yates, and N. J. Freeman, Nucl. Phys. **A94**, 177 (1967).

<sup>4</sup> R. G. Stokstad, I. Hall, G. D. Symons, and J. de Boer, Nucl. Phys. **A92**, 319 (1967).

<sup>5</sup> P. H. Stelson, W. T. Milner, J. L. C. Ford, Jr., F. K. McGowan, and R. L. Robinson, Bull. Am. Phys. Soc. **10**, 427 (1965).

<sup>6</sup> G. R. Schilling, R. P. Scharenberg, and J. W. Tippie, Phys. Rev. Letters **19**, 318 (1967).

<sup>7</sup> J. J. Simpson, U. Smilansky, and P. Wurm, Phys. Letters **27B**, 633 (1968).

$\dagger$  Work supported by the National Science Foundation.

\* Present address: Physics Department, University of Boulder, Boulder, Colo.

<sup>1</sup> J. E. Glenn and J. X. Saladin, Phys. Rev. Letters **19**, 33 (1967).

niques. The results of these various approaches are partly inconsistent. We have, therefore, complemented our earlier experiments on Cd<sup>114</sup> with additional data, using O<sup>16</sup> as well as He<sup>4</sup> beams. We find that all our results are consistent with each other and with the results of Refs. 2-6, but in contradiction with the results of Ref. 7. In this paper, we give a detailed description of the experimental techniques, the method of data evaluation, and a discussion of various effects which might affect the results. We feel that a detailed discussion of the experiment is well in order, since the quadrupole moments of the first 2<sup>+</sup> states of even-even nuclei play such a crucial role in our understanding of the structure of these nuclei.

## II. EXPERIMENTAL PROCEDURE

### A. Summary of Relations

The theory of the reorientation effect has been discussed extensively elsewhere.<sup>8</sup> Even though the final analysis is performed by means of the coupled channels code of Winther and de Boer,<sup>8</sup> it is useful as a point of departure to consider the second-order expression for the excitation probability  $P_{0^+ \rightarrow 2^+}$  of the first 2<sup>+</sup> state,

$$P_{0^+ \rightarrow 2^+} = F(\theta, \xi, \eta, A_1, Z_1, A_2, Z_2) B(E2, 0 \rightarrow 2^+) \times \left( 1 + 1.32 \frac{A_1}{Z_2} \frac{\Delta E_{\text{MeV}}}{1 + (A_1/A_2)} Q_{2^+} K(\xi, \theta) + O(Q_{2^+}^2) \right) \simeq d\sigma_{2^+} / d\sigma_{\text{Rutherford}}, \quad (1)$$

where  $F(\theta, \xi, \eta, A_1, Z_1, A_2, Z_2)$  and  $K(\xi, \theta)$  are functions which can be evaluated from existing tables,<sup>8</sup>

$$q_1 = \frac{P_{0 \rightarrow 2}(A_1)}{P_{0 \rightarrow 2}(A_1')} = \frac{F(\theta, \xi, \eta, A_1 \dots)}{F(\theta, \xi', \eta', A_1' \dots)} \frac{1 + 1.32(A_1/Z_2)[\Delta E / (1 + A_1/A_2)] Q_{2^+} K(\xi, \theta)}{1 + 1.32(A_1'/Z_2)[\Delta E / (1 + A_1'/A_2)] Q_{2^+} K(\xi', \theta)} \quad (4a)$$

for measurements of type (a), or from

$$q_2 = \frac{P_{0 \rightarrow 2}(\theta)}{P_{0 \rightarrow 2}(\theta')} = \frac{F(\theta, \xi, \eta \dots)}{F(\theta', \xi, \eta \dots)} \frac{1 + 1.32(A_1/Z_2)[\Delta E / (1 + A_1/Z_2)] Q_{2^+} K(\xi, \theta)}{1 + 1.32(A_1/Z_2)[\Delta E / (1 + A_1/Z_2)] Q_{2^+} K(\xi, \theta')} \quad (4b)$$

for measurements of type (b). Either type of measurement is in this approximation independent of the absolute value of  $B(E2, 0 \rightarrow 2)$ . (A statement in Ref. 7 to the contrary is incorrect.) In the present experiment, both types of measurements have been performed, using O<sup>16</sup> ions and  $\alpha$  particles.

### B. Experimental Arrangement

The 42-MeV O<sup>16</sup> beam carrying a charge of +6e was obtained from the University of Pittsburgh Tandem Accelerator operating in the two-stage mode. The intensity of the analyzed O<sup>16</sup> beams was typically

$A_1$  and  $A_2$  are the masses in amu of the projectile and target nuclei, respectively, and  $Z_1$  and  $Z_2$  are the corresponding charges in units of  $e$ . The symbol  $B(E2, 0 \rightarrow 2^+)$  represents the reduced electric quadrupole transition probability between the ground state and the first 2<sup>+</sup> state;  $\Delta E_{\text{MeV}}$  is the excitation energy of the first 2<sup>+</sup> state and  $Q_{2^+}$  is its static quadrupole moment in units of  $e \cdot \text{barns}$ .

The adiabaticity parameter  $\xi$  is given by

$$\xi = a\Delta E / \hbar v, \quad (2)$$

where  $a$  is half the distance of closest approach in a head-on collision and  $v$  is the projectile velocity at infinity. The parameter  $\eta$  is defined by

$$\eta = a/\lambda, \quad (3)$$

where  $\lambda$  is the de Broglie wavelength of the projectile at infinity. The last term in Eq. (1) is of the order of  $Q_{2^+}^2$  and can in the present discussion be neglected. The function  $K(\xi, \theta)$  is given in Fig. 10 and Tables 7 and 8 of Ref. 8. It depends very weakly on  $\xi$  and hence on the bombarding energy, but it is strongly dependent on the scattering angle. One notices, furthermore, that the second term in Eq. (1) is roughly proportional to the mass of the projectile. The quadrupole moment can thus be determined in two ways: (a) by measuring the excitation probability as a function of the projectile type, keeping the geometry fixed (i.e., using at least two different projectiles  $A_1$  and  $A_1'$ ), or (b) by varying the scattering angle, keeping the projectile type fixed (i.e., performing the measurements at two different angles  $\theta$  and  $\theta'$ ). The quadrupole moment is obtained from the ratio

about 0.6  $\mu\text{A}$ , that of the  $\alpha$  beam  $\sim 0.3 \mu\text{A}$ . The evaluation of the data, particularly for experiments of type (a), depends quite sensitively on a precise knowledge of the beam energy. The energy calibration of the beam-analyzing magnet was originally carried out using the C<sup>12</sup>( $p, p$ )C<sup>12</sup> resonance at  $14.233 \pm 0.008 \text{ MeV}$  and the threshold of the C<sup>13</sup>( $p, n$ )N<sup>13</sup> reaction at 3.2357 MeV. In order to exclude systematic deviations in this calibration for various beams, separate calibrations were carried out for  $\alpha$  beams and the O<sup>16</sup> beam. The  $\alpha$ -beam calibration was performed by comparing the energies of  $\alpha$  particles scattered from Os<sup>192</sup> at a scattering angle of 20° with the energies of Po<sup>210</sup> and Cf<sup>252</sup> sources, using the Enge split-pole spectrograph. It should be noted that this calibration is independent of the calibration of the spectrograph

<sup>8</sup> J. de Boer and J. Eichler, in *Advances in Nuclear Physics*, edited by M. Baranger and E. Vogt (Plenum Press, Inc., New York, 1968), Vol. 1.

itself. From this measurement it is believed that the energy of the  $\alpha$  particles used in this experiment is known to within  $\pm 2$  keV.

The calibration for  $\text{O}^{16}$  beams was carried out by means of the  $d(\text{O}^{16}, n)\text{O}^{17}$  reaction, whose threshold is at 14.522 MeV. Using  $3^+$ ,  $4^+$ , and  $5^+$  beams, it was possible to calibrate the analyzing magnet at 36.0718, 27.0534, and 21.6423 MHz. The frequency corresponding to 42 MeV  $\text{O}^{16}$  of charge  $+6e$  is 30.6696 MHz, and this energy is believed to be known to within  $\pm 10$  keV. The energy of the ions after penetrating to the center of the target was taken to be the bombarding energy in the analysis. This correction was small ( $< 30$  keV) in every case.

The experimental arrangement is shown in Fig. 1. The beam was defined by a scattering slit 1.5 mm wide by 2 mm high, which was followed by an anti-scattering slit of slightly larger dimensions. The target was partly surrounded by a liquid-nitrogen-cooled copper structure in order to prevent carbon buildup on the target. Ions scattered from the target entered the split-pole spectrograph through a rectangular aperture set at 0.9 in. wide by 0.4 in. high. The zero-angle setting of the spectrograph was checked periodically by observing elastic scattering at small angles symmetric about the beam direction. The scattering angles are believed to be accurate to within  $\pm 0.15^\circ$ .

Energy-analyzed ions, carrying charges of  $+6e$ ,  $+7e$ , and  $+8e$ , were detected by three position-sensitive detectors placed in the focal plane of the spectrograph. Errors in the experimentally determined ratios  $R = d\sigma_{2+}/d\sigma_{e1}$  due to small differences in the charge-state distributions of elastic and inelastic ions were estimated in the following way: The charge-state distribution of  $\text{O}^{16}$  ions scattered from the  $\text{Cd}^{114}$  targets used in the experiment was measured as a function of the bombarding energy. The results of these measurements are shown in Fig. 2, from which it is evident that between 97 and 99% of all the scattered ions are contained in the  $6^+$ ,  $7^+$ , and  $8^+$  charge states. It is furthermore possible to estimate from Fig. 2 that the error in  $R$  due to the exclusion of charge states smaller than  $+6e$  is less than 0.2%, which is considerably lower than the statistical uncertainties ( $\sim 1\%$ ).

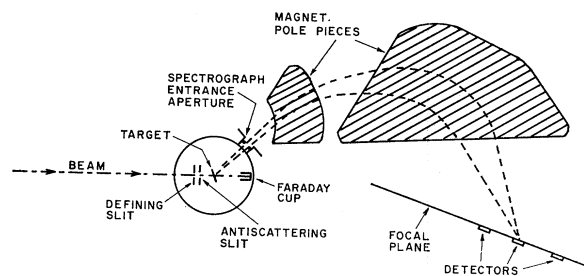


FIG. 1. Experimental arrangement. Not shown in this figure is a liquid-nitrogen-cooled cold finger surrounding the target.

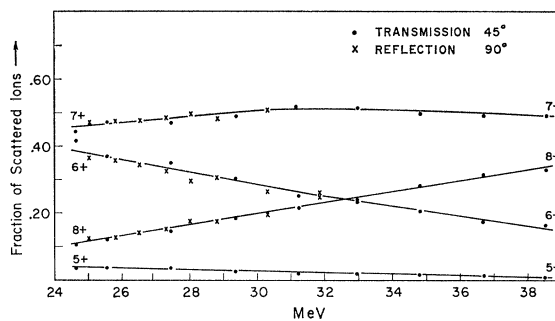


FIG. 2. Charge-state distribution of  $\text{O}^{16}$  target on a  $10\text{-}\mu\text{g}/\text{cm}^2$   $\text{Cd}^{114}$  target on a  $10\text{-}\mu\text{g}/\text{cm}^2$  carbon backing as a function of energy.

The position of the focal plane could be adjusted in order to correct for aberrations due to the large kinematic energy spread of the scattered ions. The depletion depth of the detectors was approximately  $120\ \mu$  and their sensitive area was 14 mm high by 45 mm wide. A beam spot about 2 mm high on target results in an image of about 8 mm in height at the detectors. The detectors can be moved in the vertical direction, which made it possible to experimentally determine the vertical extent of the image and the position of the three detectors with respect to it. Periodic checks were made to ensure that the detectors straddle the image.

The Cd targets were prepared by dissociating in vacuum isotopically enriched (99.09%) CdO through resistive heating. The evolving cadmium was then allowed to condense on  $10\text{-}\mu\text{g}/\text{cm}^2$  carbon backings. Targets varied in thickness from 10 to  $20\ \mu\text{g}/\text{cm}^2$  of  $\text{Cd}^{114}$ .

### C. Measurement and Analysis of Spectra

Pulses proportional to the energy  $E$  of the scattered ion and to  $X \times E$ , where  $X$  is the distance from one end of the detector to the impact point of the ion, were analyzed in a two-dimensional  $16 \times 256$ -channel mode. The spectra of inelastic and elastic events were contained in a single 256-channel subgroup, while events corresponding to ions with different energies and charge states but similar magnetic rigidity originating from scattering and reactions from the carbon backing and low-mass contaminants were found in subgroups corresponding to smaller  $E$  pulses. Typical resolutions for the  $\text{O}^{16}$  data were 200-keV full width at half maximum (FWHM). The ratio  $R_{\text{expt}} = d\sigma_{2+}/d\sigma_{e1}$  was extracted from the data after contributions from isotopic impurities had been subtracted. The subtractions were made using the Oak Ridge isotopic abundance analyses.

In the analysis of the data a correction was applied due to the fact that the measured ratio is an average over an angle interval of  $5.2^\circ$  and not the ratio corresponding to the median scattering angle. Thus the angles for which the calculations were performed were

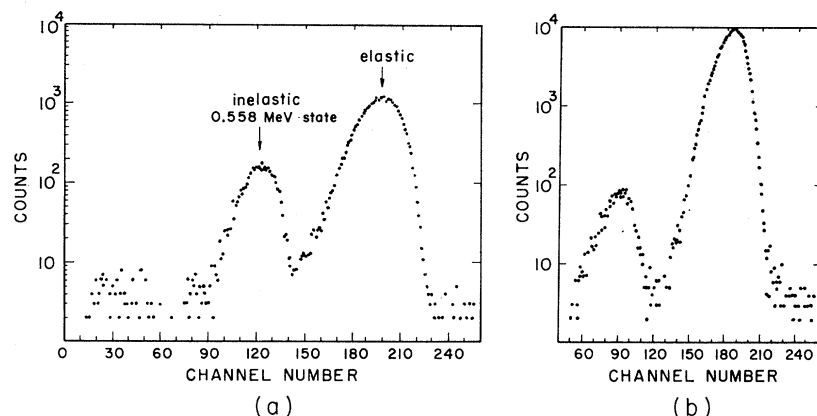


FIG. 3. Typical spectra of 42-MeV  $O^{16}$  ions scattered from  $Cd^{114}$  (a) at  $\theta_{lab} = 142.8^\circ$ , (b) at  $\theta_{lab} = 48^\circ$ .

slightly less than the angles at which the spectrograph was set. This correction is less than  $0.1^\circ$  for the angles observed, but was included in order to avoid a systematic error. The over-all error due to uncertainties in angle ( $0.15^\circ$ ) contributes uncertainties in the  $B(E2, 0 \rightarrow 2^+)$  and quadrupole moment which are about half as large as the statistical errors. Errors due to uncertainties in the bombarding energies are negligible compared with the statistical uncertainties.

### III. RESULTS

#### A. $O^{16}$ Data

Typical spectra at a forward and a backward angle are shown in Fig. 3. From these spectra, one directly obtains the ratio  $R$  of the inelastic to the elastic cross section. Note that even at the forward angle the peak-to-valley ratio for the inelastic peak is better than 20:1. The same kind of data can, in principle, be obtained by straightforward solid-state detector spectroscopy.<sup>7</sup> The acceptable solid angle in such experiments is, however, severely limited because of the large kinematic energy spread, and peak-to-valley ratios for the inelastic peaks are not as favorable as those obtained with a spectrograph.

The ratios  $R_{\text{expt}}$  as a function of scattering angle are given in Table I. The reduced transition probability  $B(E2, 0 \rightarrow 2^+)$  and the static quadrupole moment of

the first  $2^+$  state are extracted from the data by comparing the experimentally determined ratios  $R_{\text{expt}}$  with the results of Coulomb-excitation calculations in which the reduced matrix elements

$$M_{12} = \langle I_i = 0^+ || \mathfrak{M}(E2) || I_2 = 2^+ \rangle \\ = [B(E2, 0^+ \rightarrow 2)]^{1/2} \quad (5a)$$

and

$$M_{22} = \langle I_2 = 2^+ || \mathfrak{M}(E2) || I_2 = 2^+ \rangle = -Q_{2^+}/0.758 \quad (5b)$$

are treated as variable parameters. The calculations were performed by means of the Winther-de Boer Coulomb-excitation program. The program requires as input, in addition to the experimental conditions (projectile, bombarding energy, excitation energy, etc.) and the matrix elements  $M_{12}$  and  $M_{22}$ , the values for reduced matrix elements  $M_{jk}$  for all electric quadrupole interactions to be considered in the calculation. Table II lists the information about the nuclear states which was included in the computer calculation. This information was taken from the work of McGowan *et al.*<sup>9</sup> In order to apply a least-squares analysis, the results of the computer calculations were expressed in a functional form suggested by second-order perturbation theory, i.e.,

$$R_{\text{comp}}(\theta, M_{12}, M_{22}) = |M_{12}|^2 [A(\theta) + B(\theta)M_{22} \\ + C(\theta)M_{22}^2]. \quad (6)$$

TABLE I. The experimental ratios  $R_{\text{expt}} = d\sigma_{\text{inel}}(2^+)/d\sigma_{\text{el}}$  as a function of lab angle and beam energy for  $Cd^{114}$ .

$O^{16}$			$\alpha$		
Lab angle	Beam $E_n$ (MeV)	$R_{\text{expt}}$	Lab angle (deg)	Beam $E_n$ (MeV)	$R_{\text{expt}}$
45	42.0	$0.00907 \pm 0.00006$	135	8	$0.00244 \pm 0.00005$
59.4	42.0	$0.02004 \pm 0.00022$	135	8.5	$0.00338 \pm 0.00007$
89.4	42.0	$0.05259 \pm 0.00036$	135	9	$0.00438 \pm 0.00009$
119.4	42.0	$0.08456 \pm 0.00075$	135	10	$0.00699 \pm 0.00014$
133.8	42.0	$0.09548 \pm 0.00091$	135	11	$0.0106 \pm 0.0002$
134.2	42.0	$0.09702 \pm 0.00113$	135	12	$0.0147 \pm 0.0003$
142.8	42.0	$0.1020 \pm 0.0010$	135	13	$0.0198 \pm 0.0004$

<sup>9</sup> F. K. McGowan, R. L. Robinson, P. H. Stelson, and J. L. C. Ford, Nucl. Phys. **66**, 97 (1965).

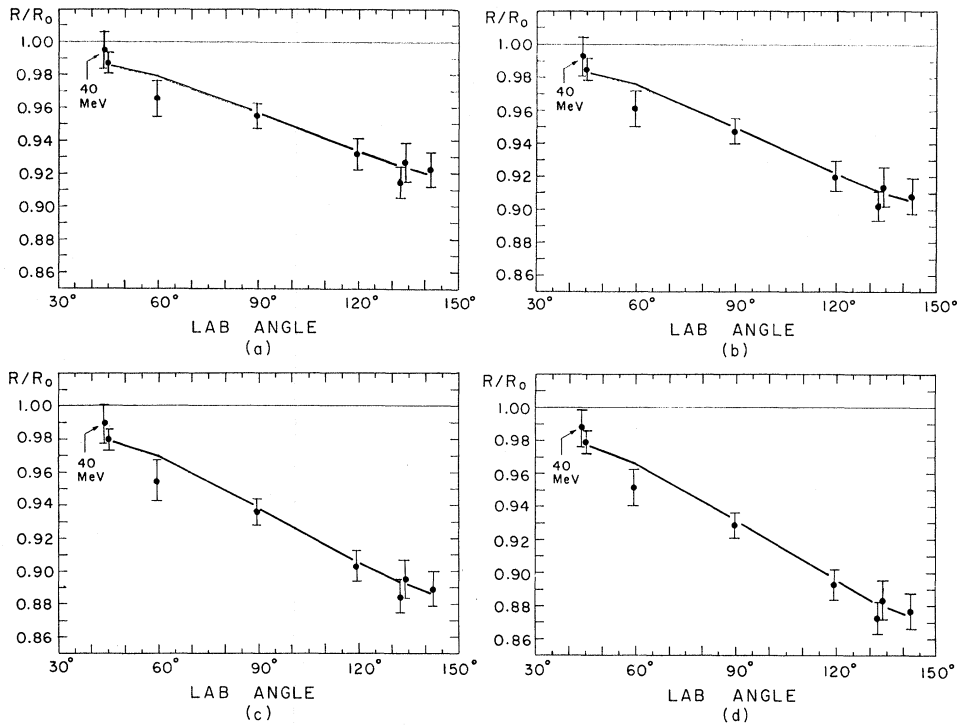


FIG. 4. Results of the least-squares-fit analysis for Cd<sup>114</sup>. The points represent the experimental ratios divided by R<sub>0</sub>. The solid lines connect values of R/R<sub>0</sub> obtained from the fit. The four fits are for the four possible combinations of the signs of the interference terms. (See Table III.)

This expression was found to reproduce the computer calculation accurately ( $\pm 0.05\%$ ) over a wide range of  $M_{22}$  values, and a change in  $M_{12}$  of a few per cent. The coefficients  $A$ ,  $B$ , and  $C$  were determined from sets of ratios  $R$  computed using different values for  $M_{12}$  and  $M_{22}$ .

It is well known that the extraction of quadrupole moments from experimental data depends quite sensitively on the relative sign of the matrix elements  $M_{jk}$ , in particular on the signs of the products  $M_{12}M_{22}M_{1Z}$ , where  $Z$  represents a  $2^+$  state different from the first excited  $2^+$  state. Unfortunately, the relative signs of these matrix elements are presently unknown and their experimental determination is difficult. The analysis of experimental data using different relative signs is

best discussed in terms of the sign of the product ( $M_{12}M_{22}M_{1Z}M_{22}$ ) which is independent of the sign convention used in defining the matrix elements. Fits corresponding to the four possible combinations of the signs of the products

$$(M_{12}M_{24}M_{14}M_{22}) \text{ and } (M_{12}M_{27}M_{17}M_{22})$$

are shown in Fig. 4. In Fig. 4 the ratios  $R_{\text{exp}}$  and the ratios  $R_{\text{comp}}$  obtained from the least-squares analysis have been divided by the ratio  $R_0$  which is calculated using the same  $B(E2, 0^+ \rightarrow 2^+)$  as obtained from the fit, but setting  $M_{22} = 0$ . Thus the deviations of the experimental points from the value  $R_{\text{exp}}/R_0 = 1$  represent the effects due to the static quadrupole moment. Values for the reduced transition probability

TABLE II. Summary of input information for the computer calculation. The matrix elements are in units of  $e \times 10^{-24} \text{ cm}^2$ . The matrix elements  $M_{12}$  and  $M_{22}$  are extracted from the data, the other matrix elements are from Ref. 9.

Level index $n$	Excitation energy (MeV)	Spin and parity	$M_{1n}$	$M_{2n}$	$M_{3n}$	Matrix elements			
						$M_{4n}$	$M_{5n}$	$M_{6n}$	$M_{7n}$
1	0.0	0 <sup>+</sup>	0	$M_{21}$	0	+0.09	0	0	+0.09
2	0.5578	2 <sup>+</sup>	$M_{12}$	$M_{22}$	+0.31	$\pm 0.84$	+1.38	+0.31	$\pm 0.34$
3	1.1331	0 <sup>+</sup>	0	+0.31	0	0	0	0	0
4	1.2084	2 <sup>+</sup>	+0.09	$\pm 0.84$	0	0	0	0	0
5	1.2822	4 <sup>+</sup>	0	+1.38	0	0	0	0	0
6	1.3049	0 <sup>+</sup>	0	+0.31	0	0	0	0	0
7	1.3629	2 <sup>+</sup>	+0.09	$\pm 0.34$	0	0	0	0	0

TABLE III. Results of the least-squares fits. Column 1 refers to the fit of Fig. 4; columns 2 and 3 give the signs of matrix-element products, i.e.,  $S_1 = \text{sgn of } M_{12}M_{24}M_{41}M_{22}$ ,  $S_2 = \text{sgn of } M_{12}M_{27}M_{71}M_{22}$ ; column 4 shows the  $B(E2, 0^+ \rightarrow 2^+)$  in units of  $e^2 \times 10^{-48} \text{ cm}^2$ ; column 5 gives the  $B(E2, 0 \rightarrow 2^+)$  values corrected for the effect of screening (see Sec. III); column 6 gives the quadrupole moment of the first  $2^+$  state in units of  $e \times 10^{-24} \text{ cm}^2$ ; and column 7 gives the value of the quadrupole moment corrected for quantum-mechanical effects.

Fit No.	$S_1$	$S_2$	$B(E2, 0^+ \rightarrow 2^+)$	$B(E2, 0^+ \rightarrow 2^+)$ corrected for screening	$Q_{2+}$	$Q_{2+}$ including quantum-mechanical correction
4a	+	+	$0.563 \pm 0.017$	$0.560 \pm 0.017$	$-0.45 \pm 0.09$	$-0.43 \pm 0.09$
4b	+	-	$0.562 \pm 0.017$	$0.559 \pm 0.017$	$-0.52 \pm 0.09$	$-0.50 \pm 0.09$
4c	-	+	$0.561 \pm 0.017$	$0.558 \pm 0.017$	$-0.64 \pm 0.09$	$-0.61 \pm 0.09$
4d	-	-	$0.561 \pm 0.017$	$0.558 \pm 0.017$	$-0.71 \pm 0.09$	$-0.68 \pm 0.09$

$B(E2, 0^+ \rightarrow 2^+)$  and the static quadrupole moment  $Q_{2+}$  obtained from the least-squares analysis are shown in Table III. The errors quoted for the quadrupole moment and the  $B(E2, 0^+ \rightarrow 2^+)$  values represent the standard deviations obtained from the least-squares analysis. The corresponding errors for the  $B(E2, 0^+ \rightarrow 2^+)$  values are 1.5%. We prefer to quote an uncertainty for the  $B(E2, 0^+ \rightarrow 2^+)$ 's of twice that, i.e., 3%, since even with peak to valley ratios of 20:1 (for the inelastic peak) there exists an ambiguity of 1 to 2% in background subtraction. For less favorable ratios, this ambiguity increases accordingly. A consistent evaluation of the data, however, does not affect the angular dependence of the ratios  $R$ , since the peak-to-valley ratios are roughly the same at forward and backward angles. The quadrupole moments should therefore not be affected by this ambiguity.

Table IV summarizes the results of all groups. Where available, the values corresponding to the two extreme sign choices for the interference term are shown. There is within the uncertainties of the evaluation rather good agreement in the value of the quadrupole moments, except for the recent results of Ref. 7. The absolute values for  $Q_{2+}$  of Ref. 4 are somewhat larger than our result. This has been attributed by the authors to attenuation of the  $\gamma$ -particle angular correlation which occurs if thin target backings are

used.<sup>10</sup> This attenuation has recently been measured by Rodgers *et al.*,<sup>10</sup> and the data of Ref. 4 were correspondingly corrected. The new value for the quadrupole moment corresponding to  $(M_{12}M_{14}M_{42}M_{22})$  positive is  $Q_{2+} = -0.35e \text{ b}$ <sup>11</sup> which is in good agreement with our corresponding value  $Q_{2+} = (-0.45 \pm 0.09)e \text{ b}$ . The measurements of Refs. 5 and 6 were performed with thick targets<sup>12</sup> for which the angular correlation seems to be unperturbed.

Our  $B(E2, 0 \rightarrow 2^+)$  value is in good agreement with a recent precision measurement of Milner *et al.*<sup>13</sup> in which 2.7- and 3-MeV protons were used. The discrepancy in the  $B(E2, 0 \rightarrow 2^+)$  values of Refs. 3 and 4 can be attributed to the difficulties associated with absolute determinations of  $B(E2, 0 \rightarrow 2^+)$  values from particle- $\gamma$ -coincidence experiments. The discrepancy between our  $B(E2, 0 \rightarrow 2^+)$  values and those of Ref. 7 is more serious, since both experiments are based on inelastic scattering. Simpson *et al.* measured  $d\sigma_{\text{inel}}/d\sigma_{\text{el}}$  for 36.2-MeV  $\text{O}^{16}$  ions scattered by  $170^\circ$  and for  $\alpha$  particles scattered by  $135^\circ$  at energies between 8.5-10 MeV using solid-state detector spectroscopy.

## B. $\alpha$ Data

In order to investigate this discrepancy, we performed a similar experiment with  $\alpha$  particles using the

TABLE IV. Summary of the results of various groups. When available, minimum and maximum values are listed corresponding to the two extreme sign choices for the interference terms.

	$Q_{\text{min}}(e, \text{b})$	$Q_{\text{max}}(e, \text{b})$	$B(E2, 0^+ \rightarrow 2^+)$ ( $e^2 \text{b}^2$ )
Skostad <i>et al.</i> <sup>a</sup>	$-0.85 \pm 0.14$	$-0.59 \pm 0.14$	$0.56 \pm 0.045$
Corrected for angular correlation perturbation <sup>b</sup>	$-0.58$	$-0.35$	
Stelson <i>et al.</i> <sup>c</sup>		$-0.6 \pm 0.2$	
Milner <i>et al.</i> <sup>d</sup>			$0.576 \pm 0.023$
Simpson <i>et al.</i> <sup>e</sup>		$-0.49 \pm 0.23$	$0.48$
Schilling <i>et al.</i> <sup>f</sup>		$-0.64 \pm 0.19$	
Present work	$-0.71 \pm 0.1$	$-0.45 \pm 0.1$	$0.56 \pm 0.017$
Simpson <i>et al.</i> <sup>g</sup>	$+0.05 \pm 0.27$	$+0.21 \pm 0.28$	$0.509 \pm 0.08$

<sup>a</sup> Reference 4.

<sup>b</sup> Reference 11.

<sup>c</sup> Reference 5.

<sup>d</sup> Reference 13.

<sup>e</sup> Reference 3.

<sup>f</sup> Reference 6.

<sup>g</sup> Reference 7.

<sup>10</sup> J. D. Rodgers, J. Gastebois, A. M. Kleinfeld, S. G. Steadman, and J. de Boer, *Bull. Am. Phys. Soc.* **14**, 122 (1969).

<sup>11</sup> J. de Boer (private communication).

<sup>12</sup> P. Stelson and R. P. Scharenberg (private communication).

<sup>13</sup> W. T. Milner, F. K. McGowan, P. H. Stelson, R. L. Robinson, and R. O. Sayer (unpublished).

spectrograph and position-sensitive detectors. It proved to be quite difficult to measure the small excitation probabilities with the required precision. Figure 5 shows some experimental spectra obtained with the spectrograph. The targets varied in thickness from 20 to 60  $\mu\text{g}/\text{cm}^2$  (on 20- $\mu\text{g}/\text{cm}^2$  carbon backings). The energy resolution was between 17- and 50-keV FWHM depending on bombarding energy and target thickness. At energies below 9 MeV, the accuracy of the data is limited by ambiguities in background subtraction even though peak-to-valley ratios for the inelastic peak were better than 15:1. Above 9 MeV, peak-to-

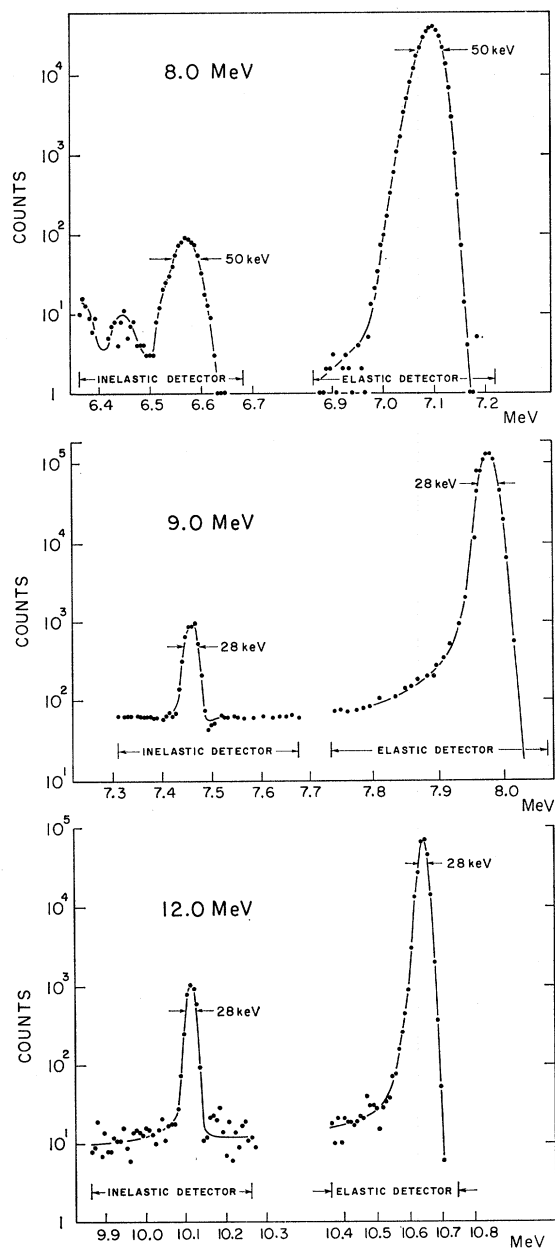


FIG. 5. Spectra of  $\alpha$  particles scattered from Cd<sup>114</sup>.

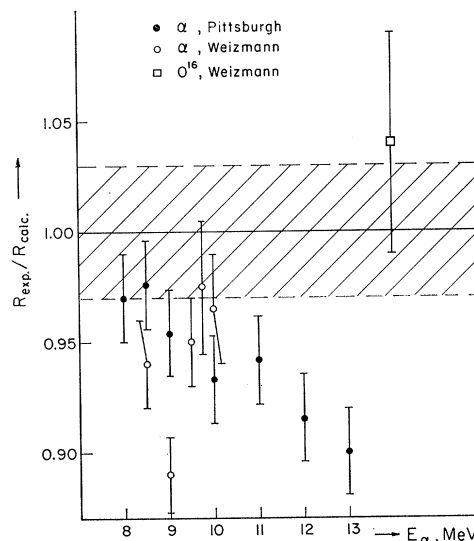


FIG. 6. Measured excitation probability divided by the calculated excitation probability using the  $B(E2, 0 \rightarrow 2^+)$  and  $Q_{2^+}(-0.45 \text{ e b})$  deduced from the O<sup>16</sup> data.

valley ratios were better than 50:1, and the accuracy of the data is limited by statistics.

The results of these measurements are summarized in Table I and Fig. 6. The latter shows the ratio  $q$  of the measured excitation probability to that calculated by using the  $B(E2, 0 \rightarrow 2^+)$  and  $Q_{2^+}$  deduced from our oxygen data.

The  $\alpha$  data should be within the shaded band in order to be consistent with the O<sup>16</sup> results. The open circles represent the results of Ref. 7; the full circles are our results. The most conspicuous feature of our data is the decrease of the ratio  $q$  with increasing bombarding energy. This trend is in agreement with the  $\alpha$  data of Skostad *et al.*<sup>4</sup> and might indicate that above 9 MeV, and possibly even lower, excitation via nuclear interaction comes into play and interferes destructively with Coulomb excitation. The 8- and 8.5-MeV points are consistent with our oxygen data. It might appear somewhat surprising that non-Coulomb interactions should become manifest at such low energies, the Coulomb barrier being at about 16 MeV. We are at present investigating this question both experimentally and by means of DWBA calculations.

In connection with the somewhat unexpected behavior of the  $\alpha$  data, it is worth mentioning that experiments with 53-MeV O<sup>16</sup> ions and 12-MeV  $\alpha$  particles on the isotopes of Os which are in progress give very consistent  $B(E2, 0 \rightarrow 2^+)$  values. Figure 6 shows that our results differ somewhat from those of Ref. 7, particularly at the lower energies.

Also included in Fig. 6 is the only O<sup>16</sup> measurement of Ref. 7, which is within its rather large uncertainty (5%) consistent with our oxygen data.

A  $\chi^2$  test using all the data of Ref. 7 leads to  $\chi^2$

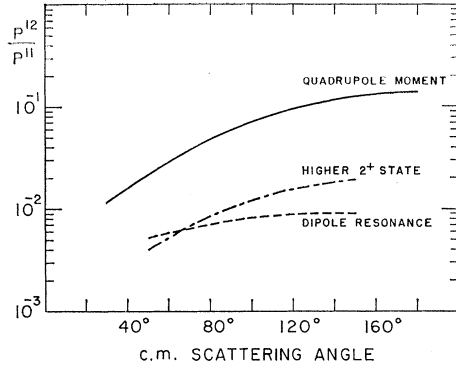


FIG. 7. Deviations from first-order perturbation theory (a) due to the quadrupole moment of the first  $2^+$  state, assuming  $Q_{2^+} = -0.758e b$ ; (b) due to the giant dipole resonance, assuming  $\eta_0 = 0.1$ ; (c) due to the second  $2^+$  state in Cd.

= 15.2 for 4 degrees of freedom [i.e., six data points minus two parameters:  $B(E2, 0 \rightarrow 2^+)$  and  $Q_{2^+}$ ] corresponding to a confidence level of  $\sim 1\%$ . The analogous result for our  $O^{16}$  data is  $\chi^2 = 4.3$  for 6 degrees of freedom, corresponding to a confidence level of 60%.

#### IV. VIRTUAL EXCITATION VIA GIANT DIPOLE RESONANCE

It has been pointed out by Eichler<sup>14</sup> that virtual excitation via the giant dipole resonance could produce effects similar to those produced by  $Q_{2^+}$ . The size of this effect depends on the nuclear structure parameter  $\eta_0$  defined by the relation<sup>15</sup>

$$\left(\frac{5}{2}\right)^{1/2} \eta_0 \sum_n \frac{\langle 0 || \mathfrak{N}(E1) || n \rangle \langle n || \mathfrak{N}(E1) || 0 \rangle}{E_n - E_i} \equiv \sum_n \frac{\langle 0^+ || \mathfrak{N}(E1) n \rangle \langle n || \mathfrak{N}(E1) || 2^+ \rangle}{E_n - E_i}, \quad (7)$$

in which  $\mathfrak{N}(E1)$  represents the electric dipole moment operator and the index  $n$  refers to the  $1^-$  states of the giant dipole resonance. Several theoretical estimates<sup>16,17</sup> give  $\eta_0 \simeq 0.11$ .

The deviation from first-order perturbation theory due to the giant dipole resonance is shown in Fig. 7 and has been calculated using the expression

$$\frac{\Delta P(E1)}{P(\text{first order})} = -1.98 \times 10^{-3} \frac{A_2 E}{Z_2(1 + A_1/A_2)} \frac{\eta_0 f_{12}}{\gamma_{if} f_{11}} \quad (8)$$

derived by Eichler. The quantity  $\gamma_{if}$  is defined by

$$B(E2, I_i \rightarrow I_f) \equiv \gamma_{if} \times 3 \times 10^{-5} A_2^{4/3} e \times 10^{-48} \text{ cm}^4,$$

and the ratio  $f_{12}/f_{22}$  has been given by Eichler as a

function of the experimental parameters. It is evident from Fig. 7 that the angular dependence of the giant dipole effect differs somewhat from that of the reorientation effect. The data were analyzed using different values for  $\eta_0$  within the range  $-1 < \eta_0 < +0.4$ . The quality of these fits as indicated by the value of  $\chi^2$  did not vary significantly over the range of values  $\eta_0$  considered. Thus it was not possible to obtain a value for  $\eta_0$  from this procedure; however, even for  $\eta_0 = -1$ , a static quadrupole moment  $Q_{2^+} < -0.2$  was needed to fit the data. The values shown in Table III were obtained assuming  $\eta_0 = 0$  and the errors quoted assume that  $|\eta_0| < 0.2$ .

#### V. QUANTUM-MECHANICAL CORRECTIONS

The computer program of Winter and de Boer, as well as the second-order expression (1), are based on a semiclassical theory of the Coulomb-excitation process. If one considers higher-order effects such as the reorientation effect, it becomes important to investigate the accuracy of the semiclassical theory compared with a quantum-mechanical treatment. Quantum-mechanical corrections have been considered by Alder and Pauli<sup>18</sup> and by Smilansky.<sup>19</sup> Alder and Pauli display their results in a convenient form in order to estimate the correction for the present data. They performed essentially exact quantum-mechanical calculations for two-level nuclei ( $0^+$  ground state and first  $2^+$  state). The excitation probability as a function of the scattering angle is then expressed in the form

$$P(\theta) = P^{(1)}(1 + C\chi_{22}), \quad (9)$$

where  $P^{(1)}$  is the exact excitation probability for  $Q_{2^+} = 0$  and

$$\chi_{22} = 8.45 \frac{A_1^{1/2} E_f^{3/2}}{Z_1 Z_2^2 (1 + A_1/A_2)^2} Q_{2^+}. \quad (10)$$

The static quadrupole moment  $Q_{2^+}$  is as usual in units of  $e b$ . The results of Ref. 18 show that the difference between  $P^{(1)}$  and  $P_{\text{semicl.}}(Q_{2^+} = 0)$  is negligible. The coefficient  $c$  can be approximately written as

$$c(\eta) = c_\infty + \Delta c \quad (11)$$

with

$$\Delta c = k/\eta, \quad (12)$$

where  $c_\infty$  is the semiclassical reorientation coefficient and  $k$  is a constant which can be evaluated from the graphs of Ref. 18. In the present experiment  $\eta = 37$  and  $\Delta c/c \simeq 0.04$ . Hence, the quadrupole moments which were obtained from the semiclassical evaluation should be reduced in magnitude by about 4%. These reduced values are shown in Table III, column 7.

<sup>14</sup> J. Eichler, Phys. Rev. **133**, B1162 (1964).

<sup>15</sup> See Ref. 8, p. 23.

<sup>16</sup> A. C. Douglas and N. McDonald, Phys. Letters **24B**, 447 (1967).

<sup>17</sup> A. Winther (private communication).

<sup>18</sup> K. Alder and H. Pauli, University of Basel, Basel, Switzerland, 1968 (unpublished).

<sup>19</sup> U. Smilansky, Nucl. Phys. **A112**, 185 (1968).



## VI. SCREENING EFFECTS

In the conventional theory of Coulomb excitation, the trajectory of the projectile is calculated under the assumption of a naked target nucleus. Under normal experimental conditions, the target nucleus, however, is surrounded by its atomic electrons. The electric potential near such a screened nucleus differs from the unscreened value. For distances which are small compared to the atomic radius, this difference is to a good approximation independent of the separation between the projectile and the target nucleus. This problem has been studied in some detail by Pearlman and Rasmussen<sup>20</sup> in the connection with  $\alpha$  decay. From their treatment, which is based on a survey of Hartree-Fock calculation by Foldy,<sup>21</sup> it is possible to derive an expression for the screening correction of the potential energy of a projectile of charge  $Z_1$  near a nucleus of charge  $Z_2$ :

$$(\Delta V)_{eV} = +Z_1(32.65 Z_2^{7/5} - 40 Z_2^{2/5}) \text{ eV.} \quad (13)$$

The effect of this correction is that for a given impact parameter the distance of closest approach for a screened nucleus is smaller than that of an unscreened nucleus. A more realistic trajectory is obtained, if the bombarding energy  $E$  (in the c.m. system) entering the calculations is replaced by  $E + \Delta V$ . In the case of Cd, Eq. (13) leads to  $\Delta V = 14$  keV for  $\alpha$  particles and  $\Delta V = 58$  keV for  $O^{16}$  ions. The main effect of the correction is to reduce the  $B(E2, 0 \rightarrow 2^+)$  values obtained from the  $O^{16}$  data by 0.6% and those from the  $\alpha$  data by 0.25%. Thus the  $\alpha$  data of Fig. 6 would be shifted upward by the difference, i.e., 0.35%. The corrected  $B(E2, 0 \rightarrow 2^+)$  values are given in Table III, column 5.

## VII. DISCUSSION

Even our lowest experimental value for  $Q_{2^+}$  ( $-0.42e$  b) is still large compared with a shell-model

expectation. Using a shell-model picture one might assume that the quadrupole moment arises from the two-proton hole configuration  $(g^{9/2})^{-2}$ . This assumption leads to  $Q_{2^+} = -0.1e$  b.<sup>22</sup> In recent years, many attempts have been made to explain the magnitude of  $Q_{2^+}$ . Higher random-phase-approximation calculations based on the pairing plus quadrupole model of the residual interaction have been performed by several authors.<sup>22-24</sup> The common result of these calculations is a quadrupole moment of the right sign but much too small in magnitude ( $-0.08e$  b).

Phenomenological models are more successful. Davydov and Ovcharenko,<sup>25</sup> using the asymmetric rotor model obtain  $Q_{2^+} = -0.53e$  b. Tamura and Udagawa<sup>22</sup> considered the mixing of one- and two-phonon states in a perturbation calculation and obtained  $Q_{2^+} = -0.42e$  b. Kumar<sup>26</sup> has proposed a transitional model in which each nuclear state is written as a combination of a vibrational state and a rotational state. This model can explain the large value of  $Q_{2^+}$  for Cd<sup>114</sup> without ruining its vibrational features.

## ACKNOWLEDGMENTS

It is a pleasure to acknowledge stimulating discussions and correspondence with Professor K. Alder and Professor J. de Boer, as well as Dr. M. Simonius. We are very much indebted to J. Kerns, S. Lane, and T. Saylor for extensive help in data taking. We want to thank Professor J. McGruer for much helpful advice on questions concerning the accelerator. The experiment would not have been possible without the competent and dedicated efforts of our technical staff. The computer calculations were performed at the University of Pittsburgh Computation Center which is partially supported by the National Science Foundation.

<sup>22</sup> T. Tamura and T. Udagawa, *Phys. Rev.* **150**, 783 (1966).

<sup>23</sup> B. Sorenson, *Phys. Letters* **21**, 683 (1966).

<sup>24</sup> Mitsuo Sano, Crocker Nuclear Laboratory, University of California, Davis, Report, 1967 (unpublished).

<sup>25</sup> A. S. Davydov and V. I. Ovcharenko, *Yadern. Fiz.* **7**, 57 (1968) [English transl.: *Soviet J. Nucl. Phys.* **7**, 41 (1968)].

<sup>26</sup> K. Kumar, *Bull. Am. Phys. Soc.* **12**, 544 (1967).

<sup>20</sup> I. Pearlman and J. O. Rasmussen, in *Handbook der Physik*, edited by S. Flügge (Springer-Verlag, Berlin, 1957), Vol. 42, p. 151.

<sup>21</sup> L. L. Foldy, *Phys. Rev.* **83**, 397 (1951).